Solar Polar Sail mission: report of a study to put a scientific spacecraft in a circular polar orbit about the sun

Bruce E. Goldstein, Andrew Buffington, Alan C. Cummings, Richard R. Fisher, Bernard V. Jackson, et al.

Bruce E. Goldstein, Andrew Buffington, Alan C. Cummings, Richard R. Fisher, Bernard V. Jackson, Paulett C. Liewer, Richard A. Mewaldt, Marcia Neugebauer, "Solar Polar Sail mission: report of a study to put a scientific spacecraft in a circular polar orbit about the sun," Proc. SPIE 3442, Missions to the Sun II, (2 November 1998); doi: 10.1117/12.330265

SPIE.

Event: SPIE's International Symposium on Optical Science, Engineering, and Instrumentation, 1998, San Diego, CA, United States

A Solar Polar Sail Mission: Report of a Study to Put a Scientific Spacecraft in a Circular Polar Orbit about the Sun

Bruce E. Goldstein[a], Andrew Buffington[b], Alan C. Cummings[c], Richard Fisher[d], Bernard V. Jackson[b], Paulett C. Liewer[a], Richard A. Mewaldt[c], Marcia Neugebauer[a]

[a]Jet Propulsion Laboratory, Pasadena, CA 91109
[b] CAS, Univ California San Diego, La Jolla, CA 92093
[c]California Institute of Technology, Pasadena, CA 91125
[d]NASA/Goddard Space Flight Center, Greenbelt, MD 20768

ABSTRACT

The Solar Polar Sail Mission uses solar-sail propulsion to place a spacecraft in a circular orbit 0.48 AU from the Sun with an inclination of 90°. The spacecraft's orbit around the Sun (4 months period) is in 3:1 resonance with Earth phased such that the Earth-Sun-spacecraft angle ranges from 30° to 150°. The polar view will further our understanding of: (1) the global structure and evolution of the corona, (2) the initiation, evolution, and propagation of coronal mass ejections; (3) the acceleration of the solar wind; (4) the interactions of rotation, magnetic fields, and convection within the Sun; (5) the acceleration and propagation of energetic particles; and (6) the rate of angular momentum loss by the Sun. Candidate imaging instruments are a coronagraph, an all-sky imager for following mass ejections and interaction regions from the Sun to 1 AU, and a disk imager. A lightweight package of fields and particle instruments (plasma spectrometer, magnetometer, energetic particle telescopes) is included. A mission using a 158 m square sail with an effective areal density of 6 g/m^2 would cost approximately $250-300M(FY97) for all mission phases, including the launch vehicle. This mission depends on the successful development and demonstration of solar-sail propulsion.

Keywords: solar sail, sail, solar wind, spacecraft, solar polar orbit, corona

1. INTRODUCTION

In 1996, NASA issued a call for proposals to study new mission concepts in space physics. One of the mission concepts selected for further definition under that program was the Solar Polar Sail Mission whose objectives would be scientific research in solar and heliospheric physics conducted from a solar polar orbit. This paper is a summary of results from that study[1]. The complete report[1] may be found on the web at http://spacephysics.jpl.nasa.gov/spacephysics/SolarPolarSail/; and also obtained in print as Jet Propulsion Laboratory Document D-15816, A Solar Polar Sail Mission, Neugebauer et al.; 1998. Both that report and this summary cover the scientific rationale and objectives of such a mission, a study of trajectory options, and a strawman payload. That information was then used as input requirements for a technical feasibility study by JPL's Advanced Projects Design Team (also known as Team X) in March and July, 1997. Their conclusions are briefly reviewed in Section 7 of the report and summary. The report and this summary conclude with a discussion of the technology development required before the Solar Polar Sail Mission can become a reality.

2. SCIENCE OBJECTIVES

All our knowledge of the Sun has been acquired from the viewpoint of the Earth, which moves over the solar latitude range of ±7.25°. From Earth, observations of features in the solar polar regions are greatly foreshortened, making the true structures of the features difficult to determine. All that is known about the structure of the corona is based on the nearly meridional views obtainable from the ecliptic. We can only surmise what views from above the solar poles would look like. One of the principal handicaps in addressing many problems in solar and heliospheric physics is that one cannot obtain high-quality data on the magnetic field in the photosphere (best observed near disk center and poorly observed near the limbs) and on processes in the chromosphere, transition region, and lower corona observed in white light, UV, EUV, and X-rays (all also poorly observed near the limbs), while also observing the related coronal processes that can only be viewed in the plane of the sky above the limbs. In other words, except in a statistical sense, it is not currently possible to follow the chain of cause and effect from magnetic phenomena at the solar surface through the corona into interplanetary space. The types of data than could be provided by a Solar Polar Sail Mission (SPSM) would allow the achievement of the objectives listed in Box 2.1 and thereby address previously unresolvable aspects of the scientific problems listed in Box 2.2.

2.1 OBJECTIVES OF A SOLAR POLAR MISSION

- For the first time, view the Sun from high latitudes
- Discover the sources, longitudinal structure, rotational curvature and time variability of coronal features
- Image the global extent and dynamic effects of coronal mass ejections
- Link particle and field observations to images of the Sun, corona, and heliosphere at all latitudes
- Determine magnetic structures and convection patterns in the Sun's polar regions
- Follow evolution of solar structures over a full solar rotation or more

Part of the SPIE Conference on Missions to the Sun II • San Diego, California • July 1998
SPIE Vol. 3442 • 0277-786X/98/$10.00

2.2 SCIENCE PROBLEMS ADDRESSED BY A SOLAR POLAR MISSION

- Global structure and evolution of the solar corona
- Acceleration of the solar wind
- Initiation, evolution, propagation, and recovery of coronal mass ejections
- Temporal evolution of active regions
- Internal structure of the Sun and generation of the solar magnetic field
- Energetic particle acceleration and propagation
- Rate of loss of solar angular momentum

2.1. Solar corona and steady solar wind

Two of the important outstanding questions[2] in solar physics are how the corona is heated to temperatures in excess of 10^6 K and how the solar wind is accelerated to speeds which range from ~300 km/s to ~800 km/s depending on the magnetic geometry of the corona. Determination of the longitudinal structure of coronal magnetic fields requires observations from above the solar poles; only with such data is it possible to determine the longitudinal extent of coronal streamers and whether or not the streamer "belt" circles the Sun without gaps. Polar views would also address the question of over what distance scale the coronal plasma loses its corotation with the Sun. A combination of observations of the azimuthal velocity with theories (e.g., reference 3) of angular momentum transfer in the accelerating wind would yield constraints on the rate of energy and momentum input for different types of solar wind flow.

A combination of coronagraph data from SPSM with that from near-Earth coronagraphs would allow the determination of the three-dimensional structures and the locations of coronal features such as streamers, plumes, and rays. For some geometries, the two lines of sight could help separate the foreground and background emission in order to study the material within the coronal holes themselves.

The study of coronal and solar-wind structures could be further enhanced by the use of an "all-sky" visible-light imager capable of mapping electron column densities between the coronagraph field of view to beyond 1 AU in order to study the evolution of coronal structures with distance, latitude, and longitude. Measurements of this type were made with the photometer system[4] flown on Helios. Combining SPSM measurements with similar near-Earth data would enable 3-D reconstructions of the electron density distribution to well beyond 1 AU.

The solar wind plasma instrument on the Ulysses spacecraft observed[5] considerable fine structure, called microstreams, in the high-speed flow from the polar coronal holes. The origin of the microstreams is not known. With SPSM it would be possible to relate the microstreams to coronal structures such as polar plumes and to features on the polar disk such as the supergranulation pattern or flaring bright points. Understanding the origin of microstreams might help choose between steady-state and impulsive models[6] of the acceleration of the solar wind in coronal holes.

2.2 Coronal mass ejections

It has been known for over a century that large solar flares are sometimes followed by strong geomagnetic activity, and the study of changes in the interplanetary medium related to solar activity has been a fruitful research topic since the beginning of the space age. Starting in the 1970's, coronal mass ejections (CMEs) have been regularly studied using both ground-based and space-based coronagraphs. From these studies it has been learned that the kinetic energy associated with CMEs is a major component of the total energy released by solar activity, exceeding the radiative energy from flares. There is currently vigorous debate about the causal relationships between CMEs and the eruption of flares or prominences; when they both occur, which starts first, and is one the cause of, or the trigger for, the other. While some progress is being made in identifying on-disk signatures of CMEs, such as the formation[7] of transient coronal holes, the end-to-end process cannot be studied for a single event unless one can observe the corona from a vantage point ~90° from Earth at the same time that one observes disk phenomena from near Earth. To understand the entire CME process, one has to observe the changes in coronal structures at the same time or shortly after the changes in the photosphere at the footpoints of the magnetic fields that thread the corona together with subsequent changes in the solar wind. One of the primary scientific objectives of SPSM is therefore to understand the physics of the initiation, evolution, and recovery phases of CMEs and related eruptive phenomena across the entire spatial domain of the events by simultaneously observing processes on the disk, in the corona, and in interplanetary space.

The reconstruction of 3-D coronal structures from 2-D images obtained from two different viewing directions will allow the determination of where the shapes of CMEs lie in the range between planar loops and spherical bubbles. With SPSM together with near-Earth observations, it would be possible to address questions such as whether or not CMEs that lead to interplanetary magnetic clouds with flux-rope geometries are more loop-like than other CMEs. SPSM would also be able to view the 3-dimensional distortion of pre-existing streamers or other features due to collisions with transient ejecta.

Theoretical models[8] indicate that CMEs may be shaped like arcades, with considerable longitudinal extent. Images of CMEs taken with the coronagraphs on SOHO have been interpreted[9] to indicate that CMEs may extend entirely around the Sun, to all longitudes; but that result could be an artifact of the integration along the line of sight and the inability of the coronagraph to distinguish foreground and background events from events near the solar limb. Using its polar perscpective, SPSM would resolve the issue by mapping the longitudinal structures of CMEs as a function of time and distance from the Sun.

2.3. Energetic Particles

The data acquired by a solar polar mission could lead to better understanding of how CMEs and flares accelerate energetic particles and how the solar wind modulates the flux of galactic cosmic rays and anomalous cosmic rays into the inner solar system.

There are two basic types of solar energetic particle (SEP) events: (1) Impulsive SEP events apparently involve the acceleration of flare-heated plasma; these events are typically rich in electrons, heavy elements such as Fe, and the rare isotope ^{3}He, and (2) Essentially all of the largest SEP events are of the "gradual" kind, apparently accelerated by shocks associated with CMEs. These events typically contain normal coronal abundances. They are observed over a much broader region of longitude than impulsive events and the highest intensities are observed when a spacecraft is directly connected to the nose of the shock in front of the CME. The time-intensity profiles observed in the ecliptic depend on the longitude of the observer. Observing events at high latitudes where the interplanetary field is more nearly radial should give qualitatively new information about the acceleration and propagation of solar energetic particles. Another mystery to be addressed by better 3-dimensional data is why most CMEs are not accompanied by energetic particles, even if the CMEs are sufficiently energetic to drive an interplanetary shock; a wider range of event geometries is required to determine the necessary conditions for energetic particle events.

Solar particle studies at 0.48 AU (See Section 3 concerning choice of radial distance) would have several important advantages over those at 1 AU. For the large gradual events caused by CMEs, most of the acceleration typically occurs close to the Sun. One possible way described recently[10] to understand this is in the interplanetary shock acceleration theory[11,12]. In this theory particles streaming away from the shock generate Alfvén waves that resonantly scatter subsequent particles, which gain energy by repeated traversal of the shock. An equilibrium is established between accelerated particles and the waves they generate. Sufficiently far from the shock the particle intensities decrease to the point that the intensity of self-generated waves is insufficient to maintain the scattering, and the particles stream freely away. The intensity peak near the shock (where this theory holds) is often observed at 1 AU at lower energies in so-called ESP (energetic storm particle) events. At sufficiently high energies the resonant scattering region does not survive to 1 AU and the ESP peak is missing. At 0.48 AU, SPSM would be within the ESP region over a much broader range of energies, where it would be able to test this theory by comparing the particle energy spectra and time-intensity profiles with in situ observations of the shock structure and the spectrum and intensity of Alfvén waves. A vantage point at 0.48 AU would also have important advantages for studying particles accelerated in impulsive solar flares because it will be much easier to relate the observed particle fluxes to features and occurrences observed in the corona by the imaging instruments because of the reduced time and angular dispersion of the particles.

With SPSM, it will also be possible to explore in greater depth those physical processes that govern the 22-year modulation of galactic and anomalous cosmic rays. We wish to know whether or not the modulations depend on the polarity of the Sun's magnetic field, on particle drifts, and/or on the intensity of waves in the polar solar wind. The recent discovery[13] that most anomalous cosmic rays with energy >10 MeV/nucleon are multiply charged implies that their latitudinal gradients should show a significant energy dependence.

Two critical parameters in the theory of transport of energetic particles in the heliosphere are the diffusion coefficients parallel and perpendicular to the direction of the interplanetary magnetic field. Those two parameters are currently not well known. From observations in the outer heliosphere and model fits to Voyager data, one can deduce[14] information about the rigidity dependence of the perpendicular mean free path, but little is known about the sensitivity of that parameter to location in the heliosphere or about the parallel mean free path. With the orbital parameters of SPSM, both the parallel and perpendicular diffusion coefficients could be determined from the radial and latitudinal gradients of anomalous cosmic rays. The latitudinal gradient would be determined repeatedly over the course of the mission, while the radial gradient could be determined by comparing low-latitude SPSM data with data obtained near Earth. On the Ulysses mission the most interesting period was the rapid latitude scan from the south pole to the north, which took ~10 months. SPSM will complete six such scans a year, all at constant radial distance, thereby removing the radial-latitude ambiguities that affected the interpretation of some of the Ulysses data.

Another investigation benefiting from SPSM is determination of the cause(s) of short-term variations in the solar wind and energetic particles such as the 26-day variations[15] in both particles accelerated in interplanetary space and galactic cosmic rays and the much faster variations that have been associated[16] with *g*-mode oscillations of the Sun. Confirmation that the solar wind and the interplanetary magnetic field transmit solar *g*-mode oscillations would provide new tools for probing the interior structure of the Sun. The SPSM orbit is highly suited for studying those oscillations as a function of latitude at constant solar distance. Other advantages of SPSM over Ulysses for addressing the problems described above lie in its closer distance

to the Sun, its better time resolution of the changes in the current sheet that regulate latitudinal gradients, and its greater number of latitude scans and polar passes.

2.4 Solar magnetic field and internal structure

Among the major processes of current concern[2] in space physics is the generation of the solar magnetic field. Because theoretical dynamo models strongly depend on the structure of convection within the Sun, we need to know how convection operates and the role of magnetic buoyancy in the solar convection zone. There are indications[17,18] that the size of chromospheric network cells is latitude dependent and some theories of solar convection predict a latitude dependence, but proof of such models require direct observations of the polar regions. Observations of the supergranulation and of magnetic and/or velocity fields from above the solar poles would thus provide new data important to untangling the interrelationships of heat flux, convection, solar rotation, and the generation of solar magnetic fields.

There is large uncertainty in our knowledge of the strength of the magnetic field in the Sun's polar regions. Measurements of polar fields with Earth-based magnetographs are highly foreshortened, making accurate measurements difficult. Observation of the polar interplanetary magnetic field by the Ulysses spacecraft, together with models of the latitudinal expansion of the flow and field from the polar coronal holes, yields estimates of the surface polar field strength of ~20 G, which is considerably higher than the values obtained from most, but not all, magnetograph data. Direct SPSM measurements of the polar field strength by a magnetograph and a magnetometer should easily resolve the issue.

Helioseismology measurements by SPSM, based on observations of either brightness variations, magnetic fields, or velocities, could extend our knowledge of the internal structure of the Sun. Combination of Earth-based and SPSM observations could provide simultaneous data over more than a single solar hemisphere and thereby yield new information on low-order acoustic waves (*p*-modes) as well as surface gravity waves (*f*-modes). The low-order p-modes penetrate deep into the Sun's interior and may yield new clues to the apparent shortage of solar neutrinos. With polar helioseismology, better data can also be obtained on the circumpolar jet streams recently discovered with the SOHO MDI instrument and on a possible polar vortex which is postulated to reach to the bottom of the convection zone.

Finally, if SPSM were to be in its polar orbit near the time in the solar cycle when the Sun's magnetic field reverses, it could provide new insights into the reversal process. Measurement of the polar fields during that time could distinguish direct, simple rotation from the more oscillatory variations that have been hinted at from Earth-based data.

2.5 Evolution of active regions

Active regions evolve over many different time scales. For studies[19] of magnetic structures associated with CMEs an important time scale for evolutionary changes is 3 to 6 weeks. From Earth the changes in these evolving magnetic structures can be well observed for only the 9 days that an active region is within 60° of central meridian. For all of the orbits under consideration for SPSM except that at 1 AU (see Section 3), much longer viewing times would be available for those active regions at favorable solar longitudes. An active region at ±30° latitude, for example, could be observed continuously within 60° of the sub-spacecraft point for up to 23 days and also viewed from Earth before and after the spacecraft observations for up to an additional 13 days.

2.6 Loss of solar angular momentum

Although the solar wind currently carries away negligible amounts of mass and energy from the Sun, understanding the rate at which a star loses angular momentum could be applied to theories of the evolution of rapidly spinning stars with stellar winds. The global rate of loss of angular momentum is not well determined (in-ecliptic measurements are discussed in reference 20). If the final SPSM orbit has a radius of 0.48 AU (or less) as suggested later in this report, the measurements of angular momentum carried away by the solar wind should be enhanced over what can be accomplished at greater heliocentric distances because of the stronger magnetic fields, the larger tangential velocities, and the decreased effects of stream interactions.

3. MISSION ARCHITECTURE

The optimal orbit for achieving the objectives described in the previous section is a circular orbit with 90° inclination to the heliographic equator (= 83° inclination to the ecliptic). The questions that then arise are what should be the size of the orbit and how should it be phased relative to Earth. To keep the spacecraft close to the plane of the solar limbs as seen from Earth (to allow viewing of the corona along the Earth-Sun line) with no solar conjunctions (which would result in a loss of telemetry), it is desired that the period of the spacecraft orbit be in resonance with the Earth's orbit around the Sun. In other words, it is desired that the orbital period of the spacecraft be 1/n years, where n is an integer. Table 3.1 lists some of the relevant parameters for orbits with n = 1 to 4.

TABLE 3.1 SELECTED MISSION-DESIGN PARAMETERS FOR THE FIRST FOUR EARTH-RESONANCE ORBITS.

n	1	2	3	4
R, AU	1.00	0.63	0.48	0.40
Earth-Sun-S/C angle, deg	60-90	40-140	30-150	22-158
Δv, km/s	42	48	52	56
Solar sail cruise time, yr	4.7 *	4.0 *	3.8	3.2

* Assumes sailing in to 0.48 AU for the latitude cranking and then returning to final distance

As seen in Table 3.1, the orbital radii for the first four resonances are 1.00, 0.63, 0.48, and 0.40 AU for n = 1 to 4, respectively. The fourth row in Table 3.1 contains an estimate of the extremely large change in velocity, Δv, that must be imparted to the spacecraft to place it in polar orbit. What are the options for achieving such polar orbits?

• Chemical Propulsion with Planetary Gravity Assists. • Jupiter gravity assist: Such orbits have aphelion distances near Jupiter. The possibilities are limited to circular orbits at a great distance from the Sun (~5 AU) or a Ulysses-type eccentric orbit with perihelion as close to the Sun as one wishes. The current plans for the Solar Probe are based on such a trajectory. The Jupiter flyby option cannot meet the requirements for circular orbits at ≤1 AU.• Earth and/or Venus gravity assists. It is possible to obtain a 1-AU circular trajectory with an inclination of 30° to the ecliptic in 4.8 years with two Venus and two Earth gravity assists. Further Earth flybys could slowly crank the orbit to still higher inclinations, but the total mission time to reach 90° inclination is unrealistically long.

• Solar Electric Propulsion (SEP). A 5 kW SEP system can deliver a 230 kg payload to a 1 AU circular orbit with a 47^0 (heliographic) inclination in about 6.5 years using a Delta II/7925 launch vehicle. (This ignores the degradation of the solar arrays over the course of the mission.) The time to a truly polar orbit is again excessive and/or a larger, more expensive SEP system and launch vehicle would be required.

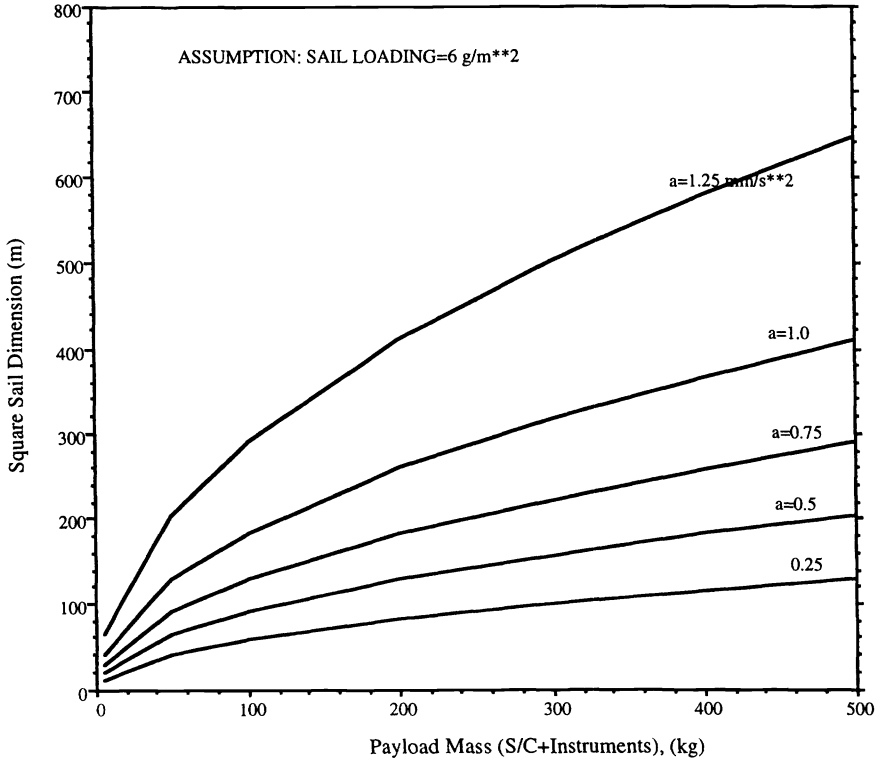

Figure 3.1 Sail size versus net spacecraft mass as a function of acceleration at 1 AU. Each curve corresponds to a different value of acceleration, a, which is given in units of mm/s^2.

• Solar Sail. Solar sail propulsion was studied in the 1970s for possible use in a mission to rendezvous with Comet Halley. The sail was huge — ~830 m on a side. Recent technological developments of smaller and lighter spacecraft subsystems and instruments make the solar-sail option more attractive than it was 20 years ago. The bottom row in Table 3.1 gives flight times for achieving circular orbits with 90° inclination using a solar sail 200 m on a side. Although the cruise times to the final orbits are still rather long, solar sail propulsion appears to be the only practical means by which the mission objectives can be achieved. With solar sail, the flight time depends on the mass to be delivered to the final orbit as well as on the mass and reflective area of the sail. The figure of merit for the sail system mass (sail + its support structure + its deployment and control mechanisms) is the effective areal density or sail loading, given in g/m^2. For a given sail loading, the trades between net or delivered mass, the acceleration, sail size, and total launched mass (the "sailcraft" mass) are shown in Figures 3.1 and 3.2 for a sail loading of 6 g/m^2

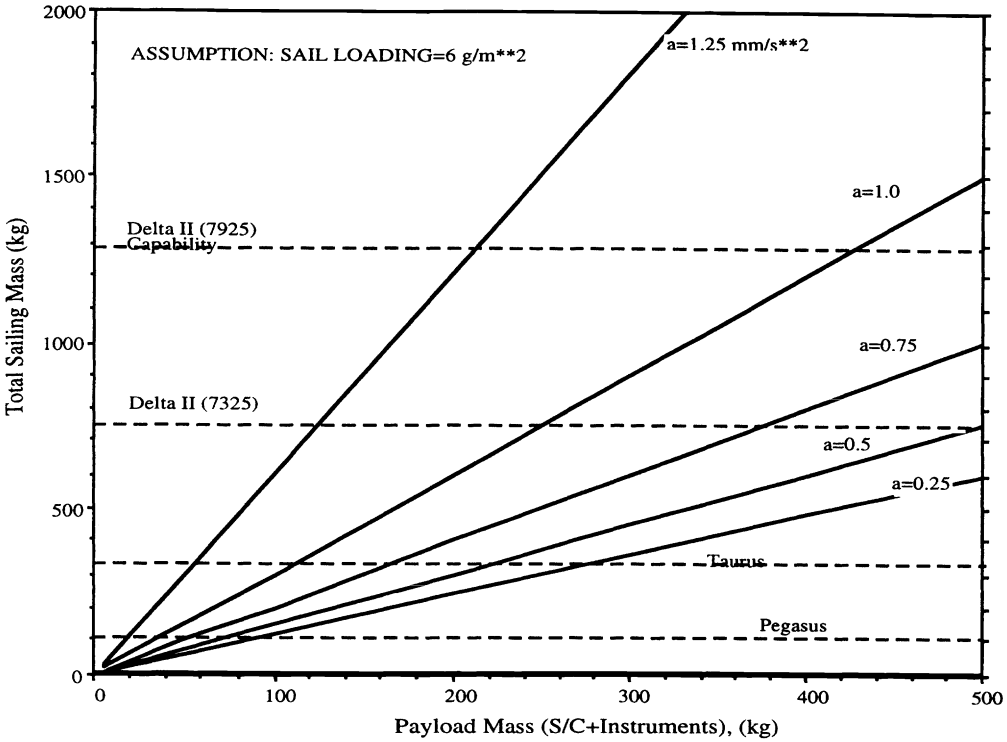

Figure 3.2 Total launched mass vs delivered spacecraft mass as a function of acceleration at 1 AU. The maximum allowable sailcraft mass depends on the launch vehicle, with limits of approximately 420, 660, 1300, and 2700 kg for the Taurus XL/Star 37FM, the Delta II/7325, the Delta II/7925, and the Atlas IIAS, respectively.

Only the n = 3 option is considered for the remainder of this study. That option was chosen because of the advantages accruing from being closer to the Sun than 1 AU (e.g., smaller optical instruments; fewer stream interactions between the Sun and point of in situ measurements of the solar wind; better capability to study the impulsive component of solar energetic particles; better resolution for separating latitudinal versus temporal effects) while keeping the spacecraft within 30° of the solar limbs for a substantial fraction of the time. Plots of some of the trajectory parameters for the n = 3 case are presented in Appendix B of Reference 1.

Table 3.2 presents flight times to an n = 3 polar orbit for several choices of sail size, sail loading, and launch vehicle. The figures are based on the 230 kg delivered mass (spacecraft + instruments) consistent with the results of the technical feasibility study described in Section 7. More information on the solar sail is given in Section 6.

TABLE 3.2 FLIGHT TIMES FOR DELIVERY OF A 230-KG SPACECRAFT TO A CIRCULAR POLAR ORBIT AT 0.48 AU

Sail Size m on a side	Sail Loading g/m^2	Sailcraft Mass kg	Launch Vehicle	Time to Orbit yrs
150 (1)	6.8 (1)	382	Taurus	5.15
158 (2)	6.0 (2)	380	Taurus	4.59
200	7.0	510	Delta II/7326	3.88
200 (3)	6.8 (3)	502	Delta II/7326	3.76
200	6.0	470	Delta II/7326	3.52
200	5.8	462	Delta II/7326	3.48

(1) DLR sail design
(2) Assumptions used for Team X study described in Section 7
(3) Assumptions used for Table 3.1

4. SCIENCE INSTRUMENTS

A strawman payload has been developed to address the objectives discussed in Section 2 in order to provide the instrument requirements as input to the technical feasibility study described in Section 7. It is envisioned that the final set of instruments for this mission would be competitively selected, so some of the detailed requirements will certainly differ from those assumed here. It is nonetheless useful to determine the broad scope of what is feasible with current or planned technology and within the limits assumed for this mission. In the current political environment, low cost and short mission duration are considered to be highly desirable attributes. For SPSM, these parameters translate into low mass and constraints on the amount of data returned. Due to the space limitations in this summary, and the fact that instrument technology may continue to evolve in the coming years, we choose not to present descriptions of the proposed instruments, but only provide

Table 4.1. Summary of instrument requirements

	Coronagraph	All Sky Camera	Disk Imager	Plasma Analyzer		Magnetometer	Energetic Part. Telescopes
				Ions	Electrons		
Mass, kg	10	3	10	3		2 + boom	2 kg
Power, w	10	4	10	12			
Pointing Control	10 arcsec	1°	60 arcsec	1°	1°	n/a	3°
Pointing Knowledge	n/a	n/a	5 arcsec (roll axis only)	0.1°	0.1°	0.1°	3°
Pointing Stability	30 arcsec/ 10 sec	0.1°/600 sec	0.01 arcsec rms @>50 Hz	0.1°/30s	0.1°/30s	0.1°/s	
Data Rate, kbps	1	1	1	0.5			
Bus Xfr Rate, Mbps	1	4	0.5	0.24	0.135	0.135	.00005
Clear FOV	Sun ± 90°	⊥ to Sun ±95°	To Sun ± tbd	Sun ± 30°	2 x (⊥ to Sun ± 80°)	n/a	Sun ± ~35°
Processing RAM	8 Mbyte	8 Mbyte	17 Mbyte	100 kbyte	102 kbyte	50 kbyte	In instrument
Processor Speed, MIP	0.3	1	1	0.02	0.02	0.01	In instrument
Thermal (operational) °C	Sensor <35	Minimize Ht Xfr across interface	Sensor <30	-20 to 50	-20 to 50	-30 to 50	-25 C to 35
Cost*, $M	12	6	18	3		2	3

* Includes prelaunch costs for science activities as well as for instruments

the information in Table 4.1 above describing the resources allocated to the experiments. For information concerning the planned experiments, please refer to Section IV of reference 1. As the All Sky Camera is not a common experiment, we describe it briefly in Appendix A at the end of this paper.

5. SPACE WEATHER APPLICATIONS

Although the 0.48 AU orbit chosen here may not be as ideal for space weather observations as a 90° inclination orbit at 1 AU, which would always be within 30° of the plane normal to the Earth-Sun Line, the 3 to 1 resonance orbit discussed in this report does put SPSM in a position to observe CMEs directed towards Earth the majority of the time. The instrumentation on SPSM could therefore make an important contribution to space weather forecasts. Moreover, SPSM would be able, much of the time, to view the development of active regions on the back side of the Sun from Earth, thereby providing the potential for longer term forecasts. From its position at 0.48 AU, SPSM would, at times, also be in a position to observe large, gradual solar energetic particle events before the nose of the shock acceleration region crosses field lines connected to Earth, and it might therefore provide up to a day's warning of large solar proton events.

For science observations alone, a single telemetry session per week is sufficient. There are two alternatives for the more frequent communications required for space weather warnings of a CME or energetic particles headed toward Earth. The first is to have continuous low-rate telemetry to a set of dedicated, nearly autonomous ground stations; a rate of ~10 bps is adequate for detecting the occurrence of Earthward-moving CMEs and/or of increased energetic proton fluxes. The second option, which has been analyzed in a bit more and costed, is based on currently evolving beacon-mode technology. A simple two-level tone is used to indicate whether or not an event has occurred, and upon detection of the occurrence of an event, a large Deep Space Net antenna is used to acquire data on the its nature. A beacon mode requires an onboard telecommunications system that can communicate with Earth 24 hours/day and at least 3 ground antennas (LEO-T, 5-meter stations, one at each DSN site, estimated cost $2M) integrated into the DSN capabilities (estimated cost $1M per station). Upon detection of an event, emergency use of a 70-m DSN antenna would command the spacecraft to transmit a special downlink. The $9M development cost for stations and their integration into the DSN might not be required if previous missions had already implemented such a beacon mode. The additional cost for operating the beacon mode is estimated to be $600k/year. These costs are not included in the cost estimates provided in Section 7.

6. SOLAR SAIL

The technical feasibility study described in the following section also requires assumptions about the nature and performance of the solar sail. The sail itself consists of a thin (≤2 μm) plastic film, such as kapton, with highly a reflecting coating on the front (toward the Sun) and a coating of thermally emitting material on the back. The strawman design for the solar polar mission is a square sail, 150 to 200 m on a side. The spacecraft is located at a hole in the center of the sail which keeps it from being overheated by reflection from the sail. A sketch of a possible configuration is shown in Figure 6.1.

There are several concepts of how to control the orientation of the sail, including:
- Control of the center-of-mass with respect to the center-of-pressure. This method, which is accomplished with a 3-axis-stabilized spacecraft bus connected to a 2-axis gimbal located on the solar sail (illustrated in Figure 7.1), was assumed for the mission feasibility study (Section VII).
- Articulation of sail segments such that the necessary imbalance of forces is provided by reefing or furling one or more quadrants of the sail (perhaps on a roller).
- Articulation of control flaps on the corners of the sail (illustrated in Figure 6.1). One analysis[21] indicates that the sail can be turned through 90° in less than an hour by feathering the flaps on one side while leaving the flaps on the other side facing the Sun.
- Surface reflectivity changes; the corners of the sail could be coated with an electrochromic material that changes its reflectivity in response to the application of an electric potential.
- Passive stabilization (camber in sail).
- Classical methods such as thrusters.

TABLE 6.1. MASS BREAKDOWN OF ONE DESIGN OF A SOLAR SAIL.

Component	Mass (kg)
Film (2 μm)	79
Booms (4 @ 106 m)	43
Deployment system	15
Stowage canister	15
Total	152
Loading factor	6.8 g/m^2

In addition to the sail itself, there must also be some support structure (spars) and mechanisms for deploying the sail at the start of the mission. Table 6.1 summarizes the mass breakdown of a design (generated by DLR, Germany) for a 150 m x 150 m sail with carbon fiber booms at 100 g/m.

The sail would be jettisoned once the final circular polar orbit is reached.

7. TECHNICAL FEASIBILITY STUDY

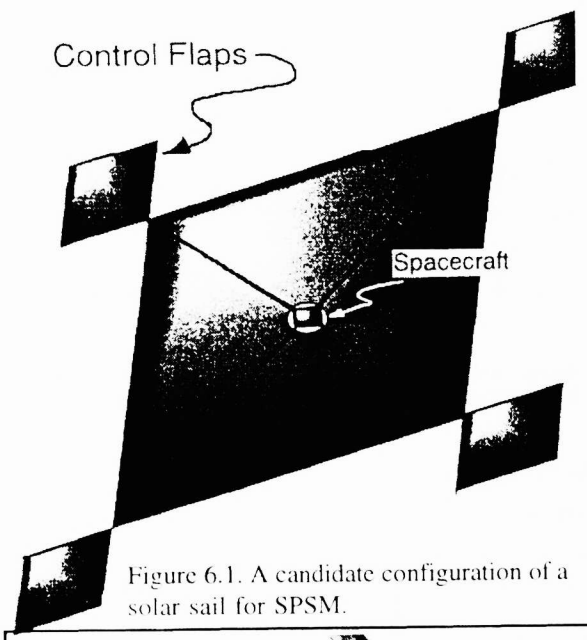

Figure 6.1. A candidate configuration of a solar sail for SPSM.

A technical feasibility study was carried out by JPL's Advanced Projects Design Team (unofficially known as Team X) on March 11-14 and July 11, 1997. The principal science requirements are given in Section IV, especially Section IV.F, while requirements arising from mission design and the use of the solar sail are given in Sections III and VI, respectively. The following system-level requirements were also determined in the discussions between the science team and Team X: • Launch date (determines technology available): 2005, • Mission duration: ≤7 years (cruise + on-orbit operations), • Mission class: B/C, • Hardware models: Protoflight spacecraft and protoflight instruments, • Redundancy: Selected, • Spares: Selected, • Parts class: Class B, Mil-883B, • Spacecraft Supplier: JPL, based on X2000 technology, • Instrument Supplier: Various, • Integration and Test Site: JPL, • Data Latency: ≤ 1 week, • Cruise Science: Not to be considered in designing the spacecraft or costing the mission, • Contingencies on mass and power: 20% on science; 30% on dry spacecraft

Figure 7.1 shows a possible configuration for the SPSM spacecraft. Once in the final polar orbit, the solar sail and its booms, container, and control boom would be jettisoned, leaving only the rather simple structures seen in the lower part of the figures.

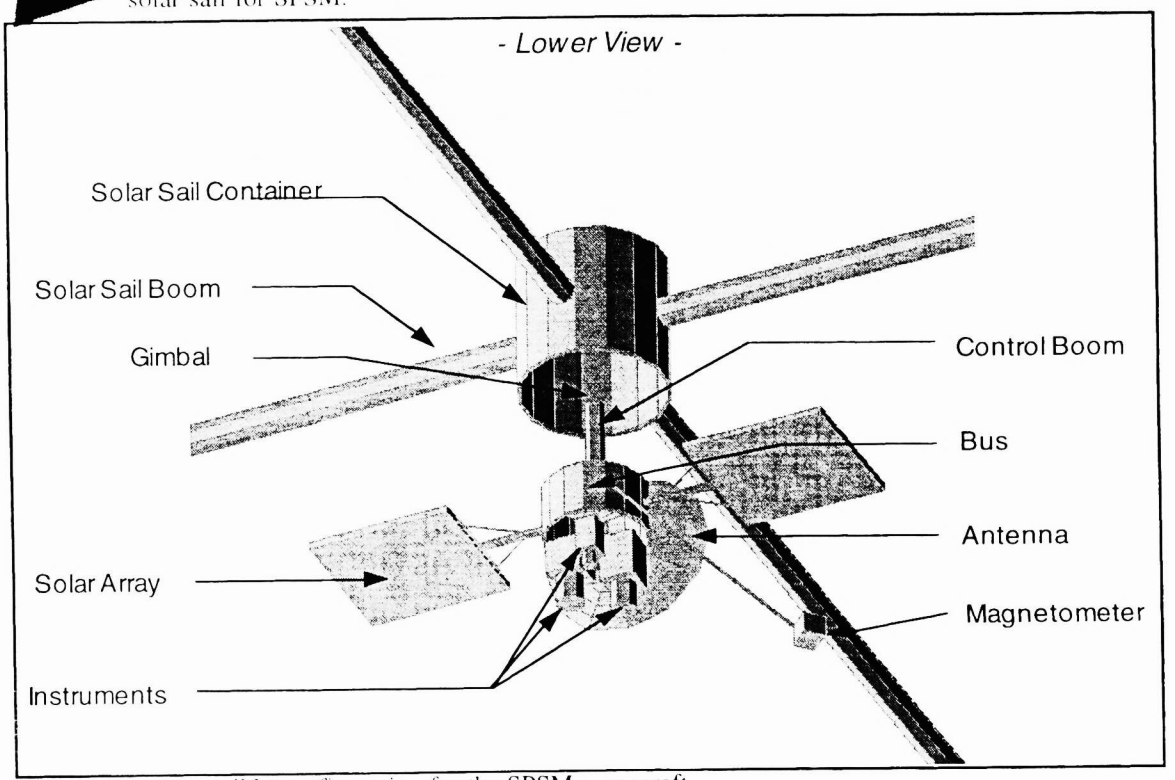

Figure 7.1. A possible configuration for the SPSM spacecraft.

Some of the spacecraft subsystem parameters that emerged from the Team X study can be summarized as follows:

Attitude Control Subsystem (ACS). The attitude control system must be capable of meeting the stringent requirements (Table 4.6 of reference 1) of SPSM's remote sensing instruments. The approach selected incorporates sun sensors, star cameras, gyros, and reaction wheels. The ACS provides coarse digital sunsensors which place the Sun in the coronagraph field of view, while the coronagraph is responsible for knowledge of fine pointing with respect to the Sun line. To meet the lifetime requirements for SPSM, the design has block redundant coarse sun sensors, star cameras, inertial reference units, interface electronics, propulsion valve drive electronics, and the sail control interface (which is not currently defined). There are internally or functionally redundant reaction wheels (4, with only 3 needed), wheel drive electronics, and single-axis drive actuator for the solar array.

Propulsion Subsystem: A hydrazine propulsion system is used to unload the reaction wheels and to maneuver the spacecraft away from the solar sail on reaching the final orbit. The wet mass of the propulsion subsystem is 22 kg.

Command and Data Handling Subsystem (C&DH). The C&DH is a block redundant system that collects data from the instruments, compresses it, stores it, and then prepares it for telemetry. The C&DH also controls critical spacecraft functions such as performing the attitude determination and control functions and decoding the uplink packets. It is block redundant.

Power Subsystem. The power for SPSM is provided by solar panels based on gallium arsenide solar array technology with a surface area of 1.1 m^2. There is also an advanced secondary Li-ion battery which will be used during launch, communications sessions, and coarse correction maneuvers.

Thermal Control Subsystem. The thermal control is basically passive, using electric heaters/thermostats to control sensitive spacecraft elements. The temperatures expected at 0.48 AU are within the qualification levels of most thermal control elements.

TABLE 7.1 SYSTEM LEVEL SUMMARY OF MASS AND POWER.

SYSTEMS WORKSHEET — ***Solar Polar Sail Mission***

Analyst: J. A. Aguilar
Date: 3/11-12,14/9; ***Directory:*** TEAMX:ACTIVE STUDIES:OTHER STUDIES:SolarPolarSail:NEW_SolarPolarSail_XL

Stabilization - cruise	3-Axis	Pointing Direction - cruise	N/A		
Stabilization - science	3-Axis	Pointing Direction - science	Solar		
P/L Pointing Control (arcsec 3 sigma)	30.0	Radiation Total Dose (krad)	72		
P/L Pointing Knowledge (aresec 3 sigma)	5.0	Redundancy	Selected	P/L Data Rate (kbps)	4
P/L Stability (arcsec/sec 3 sigma)	2.0	Mission Duration (years)	5 year flight time)	Downlink Data Rate (kb/s)	125
Pointing Requirements Driven By:	Payload	Science BER	1.00E-05	Data Storage (Gb)	10

Legend	
	Inputs from Subsystems
	Inputs from Systems
	Calculated

41.7	Mass (kg)	Mode 1 Power (W) *Science*	Mode 2 Power (W) *Xmit*	Mode 3 Power (W) *Cruise*	Mode 4 Power (W) *Launch*	Mode 5 Power (W) *N/A*	NASA TRL	Last Updated
Payload								
Instruments	30.0	33.5	3.2	3.2	0.0	0.0	5.3	3/17/97 10:05
Solar Sail *DLR (Everything Included)*	150.0	0.0	0.0	0.0	0.0	0.0		
Payload Total	180.0	33.5	3.2	3.2	0.0	0.0		
Bus								
Attitude Control	15.9	29.8	29.8	29.8	16.9	0.0	4.0	3/14/97 16:18
Command & Data	10.4	25.4	25.4	25.4	25.4	0.0	3.0	3/14/97 16:03
Power	10.4	15.8	16.1	14.0	16.7	2.2	4.0	3/14/97 15:54
Propulsion	8.7	4.0	4.0	4.0	41.0	0.0	7.0	3/14/97 14:48
Structure	54.1	0.0	0.0	0.0	0.0	0.0	6.0	3/14/97 16:15
S/C Adapter	4.2							
Cabling	13.3							3/14/97 16:15
Telecomm	13.1	12.0	44.5	28.3	28.3	0.0	5.0	3/14/97 16:11
Thermal	4.4	17.0	17.0	17.0	17.0	17.0	7.0	3/14/97 14:29
Bus Total	134.4	104.0	136.8	118.4	145.2	19.2		
Spacecraft Total (Dry)	314.4	137.5	140.0	121.6	145.2	19.2		
Mass/Power Contingency	46.3	37.9	41.7	36.2	43.6	5.8		
Spacecraft with Contingency	360.7	175.4	181.7	157.8	188.7	25.0		
Propellant & Pressurant	4.8	For S/C mass =	240.0					3/14/97 14:48
Spacecraft Total (Wet)	365.5							
L/V Adapter	14.6	*Includes 10% contingency*						3/14/97 16:15
Launch Mass	380.1	230.1 (mass w/o solar sail)						
Launch Vehicle Capability	421.0	**Taurus XL w/ Star 37FM**		Launch C3	0.5		9.0	3/12/97 9:10
				Fairing type	standard			
				Fairing dia., m	1.37			
Launch Vehicle Margin	40.9	9.7%						

Contingencies	Mass	Power
Instruments	20%	20%
Solar Sail	0%	0%
S/C, dry	30%	30%

Structure Subsystem. A JPL in-house special-purpose design was assumed in order to save mass compared to a less expensive but probably heavier general-purpose spacecraft bus procured from industry.

Telecommunications Subsystem. The length of the SPSM mission calls for a fully redundant telecom system, except for the antennas. The principal link for data return is a body-fixed, 1.5 m antenna operating at X-band radiating 13 w RF power to the DSN 70 m antenna. The data rate is 91 kbps and the link has a 3 dB data margin at a range of 1 AU from Earth. The data accumulated at an average rate of ~4 kbps can be returned in a single 8-hour pass per week. The spacecraft also has an X-band low rate link to be used during launch, cruise, and emergencies; this link is provided by three omni antennas. It supports a bit rate of ~12 bps.

Table 7.1 displays the system level mass and power summary that resulted from the Team X analysis. The total system mass at launch is 380 kg, which can be accommodated by a Taurus XL with Star 37FM launch vehicle. The mass of the instrument payload is 30 kg + 6 kg contingency. Increasing the instrument mass above that level would have a deleterious effect on the flight time to the final orbit. The instrument power is not a strongly constrained commodity because the instrument operation and most of the telecommunications occur at a solar distance of 0.48 AU.

Team X used its Deep Space Cost Model to estimate costs for this project. That model includes quasi-grass roots cost estimates for the spacecraft subsystems, the payload, mission operations, and the launch vehicle. Historical cost models are used for other mission components, including systems engineering, assembly, test, and launch operations (ATLO), project management, phases A and B, and reserves. The cost of the sail is based on an estimate from a potential vendor. Costs for developing advanced technology items (see Section 8) are not included, nor is the cost of DSN tracking time. The costs are computed in uninflated FY97 dollars. The full report[1] provides details on the calculations of the cost. To summarize, in FY97 dollars, the estimated total cost of the mission was $265M. This included 20% reserves for Phases A/B/C/D for all aspects except the launch vehicle (a Taurus XL/Star 37 costed at $38M), and 10% reserves for Phase E (post-launch operations). Team X evaluated a mission with a 158 m square sail and a cruise time of 4.6 years. The cruise could be shortened to <4 years by using a larger sail (see Table 3.2). While the cost of operations would be reduced, the launch vehicle cost would increase from $38M to $47M and the cost of the sail might increase from ~$10M to perhaps $20M.

8. TECHNOLOGY DEVELOPMENT

The Solar Polar Sail Mission is critically dependent on the successful development of solar sails. Technology that requires development and demonstration includes: • Construction of affordable sails in the 150-200 m square size range. • Achievement of loading factors in the neighborhood of 6 g/m^2, preferably less. • Successful deployment in space of a sail in the 150-200 m square size range. • Control of the sail by the sail itself, whether it be by center of pressure versus center of mass, control flaps, electrochromic variations, furling, or other means. • Long-term maintenance of reflectivity and thermal properties. Since the SPSM has no planetary encounters or other critical events, however, the mission can still be successful if there is some degradation in those properties; it will just take longer to reach the final orbit. • Software for navigation (including Earth and planetary perturbations) and sail control.

Two flight validation tests are in the planning stages. The first would test a small (30-50 m square) sail with a relatively large sail loading factor (20 g/m^2) on which the control of the sailcraft attitude would be performed using the spacecraft's cold-gas attitude control system but with the spacecraft separated from the sail by a boom. Sailcraft attitude control using the center-of-mass versus center-of-pressure technique would be carried out as an experiment. The second flight validation test would be closer to what is needed for SPSM: sail loading = 10 g/m^2, ~100 m on a side, a lightweight mechanical deployment system, and some type of photon-pressure sail control.

Substantial software development is also required for a solar sail mission, including sail control modeling and algorithms, low-thrust trajectory simulations, and navigation.

Aside from the solar sail, a few subsystem items were included in the feasibility study which are not currently funded as part of the X2000 or other programs for readiness by the start of 2003. The list includes: miniaturized reaction wheels (modified commercial reaction wheels), multi-chip module gimbal drive electronics, micro-machined silicon vibratory gyroscopes (currrently removed from the X2000 baseline), and the tiny deep space transponder (current technology cutoff date of 2003).

APPENDIX A: ALL SKY CAMERA

The purpose of the All-Sky Camera (ASC) is to trace coronal features through interplanetary space. Analogous to coronagraphs, "all-sky" photometers detect solar radiation Thomson-scattered from free electrons in the interplanetary plasma. This technique was used[22] to determine the brightness, number flux, temporal variations, speed, and spatial distribution of large-scale features propagating through the heliosphere. Those features include[23,24,25] CMEs, coronal streamers[26], interplanetary shock waves, and comets and cometary bow shocks Using a single camera, it is possible to deconvolve the density of material within those structures using different views as the structure passes the spacecraft.

The strawman ASC is based on heritage from the photometer system on the Helios mission and from a second-generation instrument called the Solar Mass Ejection Imager (SMEI). SMEI is an all-sky viewing instrument[27] currently funded by the Air Force and NASA to be built at Phillips Laboratory, at the University of Birmingham, England, and at the University of California at San Diego. It is expected to be ready for launch by the Air Force Space Test Program in the year 2000.

The important parts of the ASC are a fish-eye lens[28], a CCD detector and a baffle system. The baffle is a corral-like enclosure with five concentric knife-edge walls, with each edge progressively obscuring the previous one. The outer diameter of the baffle system is ~45 cm. The baffle reduces direct sunlight and reflections from illuminated portions of the spacecraft by a factor of 10-12 provided they are not within 90° of the normal to the instrument (i.e., the instrument provides a 2 π field of view of the corona/interplanetary medium).

10. ACKNOWLEDGMENTS

Engineering support was provided to the study by R. A. Wallace, J. Ayon, C. E. Garner, C. Sauer, C.-W. Yen, and the Advanced Projects Design Team (Team X) led by R. Bennett. A portion of this work was conducted at the Jet Propulsion Laboratory, California Institute of Technology, under contract with the National Aeronautics and Space Administration.

11. REFERENCES

1. Neugebauer, M., et al., A Solar Polar Sail Mission: Report of a Study to Put a Scientific Spacecraft in a Circular Polar Orbit about the Sun, (1998), Jet Propulsion Laboratory Document D-15816; also available electronically at the URL http://spacephysics.jpl.nasa.gov/spacephysics/SolarPolarSail/
2. Space Studies Board, National Research Council, *A Science Strategy for Space Physics,* National Academy Press, Washington, DC. 1995
3. Weber, E. J., and L. Davis, Jr.. *Astrophys. J.,* **148**: 217, 1967.
4. Jackson, B. V. and C. Leinert, *J. Geophys. Res.* **90**: 10759, 1985.
5. Neugebauer, M., B. E. Goldstein, et al., *J. Geophys. Res.* **100**: 23,389, 1995.
6. Feldman, W. C., et al., *J. Geophys. Res.* **102**: 26,903, 1997.
7. Kozuka, Y., T. Watanabe, et al., *Publ. Astron. Soc. Japan* **47**: 377, 1995.
8. Steinolfson, R. S., *J. Geophys. Res.* **97**: 10,811, 1992.
9. Brueckner, G. E., *EOS. Suppl.,* **77**: F561 (abs.)., 1996.
10. Reames, D. V., L. M. Barbier, and C. K. Ng, *Astrophys. J.* **466**: 473, 1996.
11. Lee, M. A., *J Geophys. Res.* **88**: 6109, 1983.
12. Lee, M. A. and J. M. Ryan, *Astrophys. J.* **303**, 829, 1986.
13. Mewaldt, R. A., R. S. Selesnick, et al., *Astrophys. J. Lett.* **466**: L43, 1986.
14. Cummings, A. C., E. C. Stone, and W. R. Webber, *Geophys. Res. Lett.* **14**: 174, 1987.
15. McKibben, R. B., J. A. Simpson, et al., *Space Sci. Rev.* **72:** 403, 1995.
16. Thomson, D. J., C. G. Maclennan, et al., *Nature* **376**: 139, 1995.
17. Münzer, H., et al., *Astron. Astrophys.* **213**, 431, 1989.
18. Rimmele, T., and E. H. Schröter, *Astron. Astrophys.* **221**: 137, 1989.
19. Feynman, J., *Coronal Mass Ejections, Causes and Consequences,* J. A. Jocelyn, N. Crooker, and J. Feynman, eds., Amer. Geophys. Un.: 49, 1997.
20. Pizzo, V., et al., *Astrophys. J.* **271**, 335, 1983.
21. Spilker, T., *Team X Solar Sail Polar Mission (space weather version),* Jet Propulsion Laboratory, 16 September, 1996.
22. Jackson, B. V. and C. Leinert, *J. Geophys. Res.* **90:** 10759, 1985.
23. Jackson, B. V., *Solar Physics* **100**: 563, 1985.
24. Jackson, B. V. et al., *J. Geophys. Res.* 90: 5075, 1985.
25. Webb, D. F., and B. V. Jackson, *J. Geophys. Res.* **95** 20641, 1990.
26. Jackson, B. V., *J. Geophys. Res.,* **96;** 11307, 1991.
27. Jackson, B. V., A. Buffington, et al., *Phys. Chem. Earth* **22**: 441, 1996.
28. Smith, W. J., *Modern Lens Design,* McGraw Hill, Inc., New York, 1992.